

---

Articles

---

2023-12-01

## Raman spectroscopic analysis of human serum samples of convalescing COVID-19 positive patients

Hugh Byrne

*Technological University Dublin, hugh.byrne@tudublin.ie*


Naomi Jackson

*Technological University Dublin, naomi.jackson@tudublin.ie*

Jaythoon Hassan

*National Virus Reference Laboratory, jaythoon.hassan@ucd.ie*

Follow this and additional works at: <https://arrow.tudublin.ie/creaart>

 Part of the [Biological and Chemical Physics Commons](#), [Diagnosis Commons](#), and the [Virus Diseases Commons](#)

---

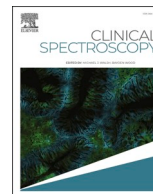
### Recommended Citation

Naomi Jackson, Jaythoon Hassan, Hugh J. Byrne, Raman spectroscopic analysis of human serum samples of convalescing COVID-19 positive patients, *Clinical Spectroscopy*, Volume 5, 2023, 100028, ISSN 2666-0547, DOI: 10.1016/j.clispe.2023.100028

This Article is brought to you for free and open access by ARROW@TU Dublin. It has been accepted for inclusion in Articles by an authorized administrator of ARROW@TU Dublin. For more information, please contact [arrow.admin@tudublin.ie](mailto:arrow.admin@tudublin.ie), [aisling.coyne@tudublin.ie](mailto:aisling.coyne@tudublin.ie), [vera.kilshaw@tudublin.ie](mailto:vera.kilshaw@tudublin.ie).



This work is licensed under a [Creative Commons Attribution-NonCommercial-No Derivative Works 4.0 International License](#).



# Raman spectroscopic analysis of human serum samples of convalescing COVID-19 positive patients

Naomi Jackson<sup>a,\*</sup>, Jaythoon Hassan<sup>b</sup>, Hugh J. Byrne<sup>a</sup>

<sup>a</sup> FOCAS Research Institute, TU Dublin, City Campus, Dublin 8, Ireland

<sup>b</sup> National Virus Reference Laboratory, University College Dublin, Belfield, Dublin 4, Ireland

## ARTICLE INFO

### Keywords:

Human Serum  
Raman spectroscopy  
COVID-19  
Convalescing  
Glutathione

## ABSTRACT

Rapid screening, detection and monitoring of viral infection is of critical importance, as exemplified by the rapid spread of SARS-CoV-2, leading to the worldwide pandemic of COVID-19. This is equally the case for the stages of patient convalescence as for the initial stages of infection, to understand the medium and long term effects, as well as the efficacy of therapeutic interventions. Optical spectroscopic techniques potentially offer an alternative to currently employed techniques of screening for the presence, or the response to infection. In this study, the ability of Raman spectroscopy to distinguish between samples of the serum of convalescent COVID-19 positive patients and COVID-19 negative serum samples, and to further analyse and quantify systemic responses, was explored. The study included serum samples of patients who had been tested for SARS-CoV-2 specific IgG and IgM responses between 25 and 134 days after the infection was identified. Both COVID-19 positive and negative groups included males and females who ranged in age from 21 to 81 years old. No correlation was apparent between the specified SARS-CoV-2 specific IgG and IgM immunoglobulin levels of the positive group, their sex, or age. Raman spectroscopic measurements were performed at 785 nm, in liquid serum, thawed from frozen, and spectra were pre-processed to remove the contribution of water, normalising to the water content. Principal components analysis of the spectral dataset over the range 400–1800  $\text{cm}^{-1}$  provided no clear indication of a difference between normal serum and SARS-CoV-2 positive serum. A selection of 5 of the samples, which were available in sufficient volume, were fractionated by centrifugal filtration, and the 100 kDa, 50 kDa, 30 kDa, and 10 kDa concentrates similarly analysed by Raman spectroscopy. Partial least squares regression analysis revealed a negative correlation between the spectral profile of the 30 kDa fractions and SARS-CoV-2 specific IgG antibody levels, potentially indicating an association with depleted glutathione levels. The study supports a potential role of Raman screening of blood serum for monitoring of SARS-CoV-2 infection, but also in longitudinal studies of disease progression, long term effects, and therapeutic interventions.

## 1. Introduction

A pneumonia outbreak of unknown origin was reported in Wuhan, China, in December 2019. Injection of respiratory samples into Vero E6 and Huh7 cell lines of human airway epithelial cells resulted in the isolation of a novel respiratory virus that was later identified by genome analysis as a novel coronavirus related to SARS-CoV and given the name severe acute respiratory syndrome coronavirus 2 (SARS-CoV-2) [1]. The World Health Organization declared a pandemic on March 12, 2020, due to the global spread of the SARS-CoV-2 virus and the rapidly escalating number of reported deaths brought on by COVID-19. The world has already paid a significant price for this pandemic, in terms of loss of

human lives, negative economic effects, and rising levels of poverty [2]. Although, at the time of writing, the worldwide spread of the virus appears to have subsided, the outbreak highlighted that there remain many knowledge gaps in our understanding of the mechanisms of viral infection, replication and host response, and shortcomings in methodologies available to analyse and characterise them. The development of rapid, automated, cost effective and reliable screening methods for viruses is paramount in the fight against disease. This is crucial to enable monitoring of disease outbreaks, and patient prognosis and treatment. Analysis of the viral load and systemic biochemical responses is also vital for monitoring disease progression and the impacts of therapeutic interventions [3,4].

\* Corresponding author.

E-mail address: [Naomi.Jackson@TUDublin.ie](mailto:Naomi.Jackson@TUDublin.ie) (N. Jackson).

<https://doi.org/10.1016/j.clispe.2023.100028>

Received 19 May 2023; Received in revised form 3 October 2023; Accepted 4 October 2023

Available online 7 October 2023

2666-0547/© 2023 Published by Elsevier B.V. This is an open access article under the CC BY-NC-ND license (<http://creativecommons.org/licenses/by-nc-nd/4.0/>).

Spectroscopic techniques such as Raman scattering and Infrared (IR) absorption are powerful analytical tools and their potential role in medical diagnostics is being increasingly explored [5–7]. These techniques provide a fingerprint of the biochemical composition of samples and can differentiate between healthy and diseased samples, as several studies have demonstrated [8–11]. Sampling of patient bodily fluids is minimally invasive and has a high compliance rate in patients. Recent studies using Raman and IR have demonstrated great potential for their use with liquid biopsy samples [12–15]. Not only can Raman and IR techniques be utilised for cancer diagnostics, they have also shown the ability for detection of viral infection. The presence of the human immunodeficiency, human papilloma, hepatitis and dengue virus have all been observed with Raman and/or IR spectroscopy [16–21], and quantitative prediction of viral loads has been demonstrated for the blood borne virus hepatitis C [22].

Recently, the potential role of spectroscopy in the global response to the COVID-19 pandemic has been discussed extensively [23–29], and it has been demonstrated that Surface Enhanced Raman Spectroscopy can be employed for the detection of the SARS-CoV-2 virus in environmental samples [30]. Barauna et al. demonstrated the potential to establish COVID-19 positivity using IR spectroscopic screening of saliva samples [31], and more recently, Wood et al. demonstrated a specificity of 82 % and sensitivity of 93 % for COVID-19 detection based on IR screening of the saliva [32]. Notably, although the diagnostic performances are comparable, the authors have commented on the validity of the results obtained by Barauna et al. [33]. The potential advantages of Raman spectroscopic screening of liquid serum samples over IR screening of dried serum samples have recently been demonstrated for the case of glucose monitoring [34,35]. Although not a blood borne virus [36], the COVID-19 immuno response resulting from SARS-CoV-2 infection is manifested in the bloodstream [37,38], and Yin et al. have recently presented a study of 177 blood serum samples, collected from 63 confirmed COVID-19 patients, 59 suspected cases, and 55 healthy individuals, reporting a classification accuracy of 0.87 for COVID-19 positive versus the suspected cases, and an accuracy of 0.90 for the COVID-19 positive cases and the healthy controls [39]. Although not explicitly discussed, the typical turn around time for such a spectroscopic screening and analysis is < 1hr, and this study clearly

demonstrates the potential of Raman spectroscopy as a rapid and effective COVID-19 screening protocol. The study employed (machine learning) support-vector machine based approaches to analysis and classification, but notably, no further analysis of the spectral profiles, or correlation with other potential biomarkers was undertaken.

This study seeks to further explore the potential of Raman spectroscopy to contribute to the continuing global effort to better understand the effects of the SARS-CoV-2 virus and the associated COVID-19 disease, by analysis of blood serum samples of convalescing COVID-19 positive patients, to explore whether spectroscopic signatures of prior infection are identifiable. The analysis will attempt to correlate any identifiable spectroscopic signatures with established systemic response biomarkers, in whole and fractionated serum samples. Potential applications in the detection and monitoring of infection, disease progression and therapeutic interventions are discussed.

## 2. Materials and methods

### 2.1. Serum and protein samples

Blood serum from 10 normal (negative for COVID-19) and 25 COVID-19 positive patients with varying SARS-CoV-2 specific IgG and IgM antibody levels were available for study. The 10 normal and 20 samples (Samples #1–20, Table 1) were purchased from RayBiotech, USA (<https://www.raybiotech.com/covid-19-patient-samples/>) and 5 (Samples #21–25, Table 1) from Cambridge bioscience, UK (<https://www.bioscience.co.uk/cpl/covid-19-human-serum-plasma>).

Throughout the manuscript, when they need to be differentiated, they will be referred to as SET A (Samples #1–20) and SET B (Samples #21–25), respectively. The blood samples were drawn from the patients between 28 January and 21 August 2020, 25–134 days post confirmation of infection by a COVID-19 positive RT-PCR, antigen, and/or antibody serology test, and the SARS CoV-2 specific IgG and IgM levels of these samples were measured by the supplier. Samples from COVID-19 patients had been inactivated with 0.5 % Triton X-100, and supplied in an EDTA treated test tube. The negative samples were taken pre COVID-19 and included 7 males and 3 females ranging in age from 18 to 65 years. Post collection, the negative samples were treated in the same

**Table 1**

Details of COVID-19 positive serum samples (n = 25) available to this study, as provided by the supplier (SET A, Samples 1–20 Supplied by Raybiotech) (SET B, Samples 21–25 supplied by Cambridge Bioscience). SARS-CoV-2 specific IgG cut off values = 15, IgM cut off values = 2 (SET A). LIASON® DiaSorin method used for IgG and IgM values of SET B.

SAMPLE #	GENDER	AGE	SARS-CoV-2 specific IgG	SARS-CoV-2 specific IgM	COVID TEST TECHNIQUE	DELAYED DAYS
1	M	52	23.3	53.05	Antibody (IgG+, IgM-)	37
2	F	21	30.4	52.19	Antibody (IgG+, IgM-)	30
3	M	59	32.84	752.304	PCR	33
4	F	71	34.58	1079.7	PCR	34
5	F	81	42.4	447.948	PCR	33
6	M	75	45.88	679.963	PCR	33
7	M	57	64.98	100.663	PCR	34
8	M	35	86.28	41.89	PCR/Antibody	32
9	F	52	89.89	1250.42	PCR	33
10	F	64	92.04	149.853	PCR	33
11	M	44	120.9	474.17	Antigen	25
12	F	56	150.28	1735.77	PCR	33
13	M	62	153.76	195.8	PCR	34
14	M	67	157.96	1625.08	PCR	33
15	M	50	188.81	259.827	PCR	34
16	F	69	209.44	63.4312	PCR	34
17	F	60	213.12	304.063	PCR	33
18	F	76	232.8	564.567	PCR	34
19	M	55	275.39	236.77	PCR	33
20	F	68	370.76	672.697	PCR	34
21	F	50	134	0.18	PCR	134
22	F	38	37.4	3.08	PCR	44
23	F	53	275	0.81	PCR	27
24	M	59	216	0.45	PCR	134
25	M	59	576	NA	PCR	24

way as the COVID-19 positive samples, with the exception of the Triton X-100 treatment. The samples were purchased in November 2020, delivered and stored as frozen. Raman spectroscopy was performed in March 2021 and in June 2021, after thawing. Note, it has previously been reported that IgG and IgM response levels to a range of antigens are stable even after 30 freeze-thaw cycles [40,41].

This study was approved by the Human Research Ethics Committee, University College Dublin.

Normal pooled serum samples were purchased from Fischer Scientific, Dublin, Ireland, and were measured using the same method as positive samples. Albumin, C-reactive protein (CRP) and glutathione were purchased from Sigma Aldrich (Arklow, Ireland) and measured as high concentration, wet pastes on glass slides.

SET B was selected for sequential fractionation, as 1 ml volumes of each sample were received, compared to 5  $\mu$ L of SET A. Varying sizes of 100 kDa, 50 kDa, 30 kDa and 10 kDa Amicon Ultra centrifuge tubes were used in order to fractionate and concentrate differing molecular size ranges within the SARS-CoV-2 positive samples. Prior to fractionation, the filters were washed following the method outlined by Bonnier et al., 2014 [42]. The washing procedure involved a cleansing of the 0.5 ml filters using 0.1 M of NaOH and centrifugation at 14,000 g for 530 min, followed by rinsing with water at the same force for 5 min, three times. When completed, the filters were centrifuged upside down to remove excess water, and were then ready to use. Fractionation was performed by adding 0.5 ml of the serum to each filter, centrifugation at 14,000 g for 30 min (allowing the filtrate to pass through, containing molecules with lower molecular weight), followed by an upside down spin at 1000 g for 2 min, to collect the concentrate. The filtrate was subsequently utilised for a further fractionation by the next filter size (from 100 kDa to 50 kDa, 30 kDa and 10 kDa). The sequential fractionation therefore resulted in samples > 100 kDa, > 50 kDa, > 30 kDa, and > 10 kDa.

## 2.2. Raman microspectroscopy

A Horiba Jobin-Yvon LabRam HR800 spectrometer with a 16-bit dynamic range Peltier cooled CCD detector was used to record the Raman spectra throughout this work. The spectrometer was coupled to a Olympus 1X71 inverted microscope and a x60 water immersion objective (LUMPlanF1, Olympus) was employed, following the previously described measurement protocol [43–45]. A 785 nm laser line was employed as source, yielding  $\sim$ 50 mW at the sample. 5  $\mu$ L of each sample was measured in the inverted geometry through a 96 well-plate with glass coverslip bottom (Thermo Fisher number 1, 0.17 mm thickness) The Raman signal was integrated for  $3 \times 15$  s over the spectral range from 400 to 3500  $\text{cm}^{-1}$ .

## 2.3. Data Preprocessing and Analysis

A general overview of multivariate pre-processing and statistical analysis techniques can be found in [46]. The raw spectra underwent pre-processing using established protocols (Matlab 2021a) before further analysis. Spectra were smoothed using a Savitzky-Golay filter of order 5, to reduce the noise, before being subjected to a background correction protocol based on Extended Multiplicative Signal Correction (EMSC [47]), specifically to remove the contributions of scattering [48] and the water of the aqueous environment [49]. Using the EMSC water subtraction protocol of Kerr et al. [50], the weighted sum of the reference water spectrum and the fitted polynomial ( $N = 10$ ) was subtracted from the spectra in the fingerprint region (400 – 1700  $\text{cm}^{-1}$ ), and, as described by Parachalil et al., the weighting co-efficient of the water was used to normalise the remaining spectral profile to the subtracted water content, to account for measurement variability due to sample repositioning and refocussing [45]. The data was not further normalised for either PCA or PLSR.

The preprocessed spectral data was analysed by Principal Components Analysis (PCA) and Partial Least Squares Regression (PLSR)

analysis, using a combination of in house scripts (Matlab 2021a) and the PLS Toolbox (Eigenvector Research, Inc., USA).

In the case of PCA, the negative and positive datasets were better balanced by including the negative samples twice in the dataset [51]. The combined datasets were mean centred, and the first 3 PCs were analysed, as they were seen to explain >95 % of the variance of the dataset.

PLSR was applied to the spectra of the SET B COVID-19 positive samples only, and regression was performed against the target variables of IgG, as listed in Table 1. Models were constructed using the specified number of LVs, chosen as the minimum number for which the Cumulative %Variance was maximised, as determined using a Leave One (Patient) Out Cross Validation.

## 3. Results

### 3.1. Demographic characteristics of patient cohort

Twenty-five serum samples from patients who were convalescing after COVID infection, and ten from pre-COVID healthy controls, were included in the study. Table 1 outlines the characteristics of the COVID positive patient group. Serum samples from 12 males ranging in age from 35 to 71 years and 13 females ranging in age from 18 to 81 years were studied. The blood samples were taken 25–134 days post infection. In the case of SET A, the levels of IgG and IgM specific for the SARS-CoV-2 spike receptor binding domain region indicate a positive antibody response if a unit number greater than cut-off values of 15 for SARS-CoV-2 specific IgG and 2 for IgM was obtained. As shown in Fig. 1(a), no correlation is observed between the specified levels of SARS-CoV-2 specific IgG and IgM, and there is no differentiation of SARS-CoV-2 specific IgG and IgM levels based on gender, and no correlation with age (Fig. 1(b)). Set B were supplied with values of SARS-CoV-2 specific IgG and IgM as measured using the LIASON® DiaSorin method, and so were not directly comparable to those of Set A.

### 3.2. Raman spectroscopic analysis of whole serum

The total protein content in human serum typically varies from 60 to 80 g/L [52]. The density of water, on the other hand is  $\sim$ 1000 g/L, and so the variations in protein content are not expected to significantly affect the water content of the serum. It is observed that the serum samples are visibly, but variably, tinted with a yellow hue, largely due to the carotenoid content, which can dominate the Raman spectrum at near resonant wavelengths such as 532 nm [53,54], and cloudy, which gives rise to a broad scattering background to the Raman spectra [55]. The EMSC protocol effectively removes the background scattering, as a polynomial, of order  $N = 10$ , as well as the specific spectrum of water, which has a peak at  $\sim$ 1640  $\text{cm}^{-1}$ , due to H-O-H scissoring vibration [56].

The Raman spectra of the COVID-19 positive serum samples are shown in Fig. 2, before (a), and after (b) preprocessing (according to protocols of Section 2.3). Note, 2 samples (#11 and #17, Table 1) yielded spectra which were obvious outliers, having significantly larger backgrounds, and were excluded from the study, reducing the number of SET A, COVID-19 positive serum samples to  $n = 18$ . No outliers were observed in the COVID-19 negative dataset.

Principal components analysis of the preprocessed spectra of the COVID-19 negative and COVID-19 positive samples (including SET A and SET B) indicates no clear differentiation between the serum samples, according to either the first (PC1 88.5 % of the observed variance), second (PC2 4.7 % of the observed variance) or third (PC3 2.7 % of the observed variance) principal components, which might be indicative of the prior infection, identified 25–134 days earlier, depending on the patient (Fig. 3(a) and (b)). The gender bias between male and female COVID-19 patient samples was examined and no differentiation between them was found, and there was no significant difference according to age, categorised as  $<$  ( $n = 8$ ) or  $>$  ( $n = 10$ ) 60 years (data not

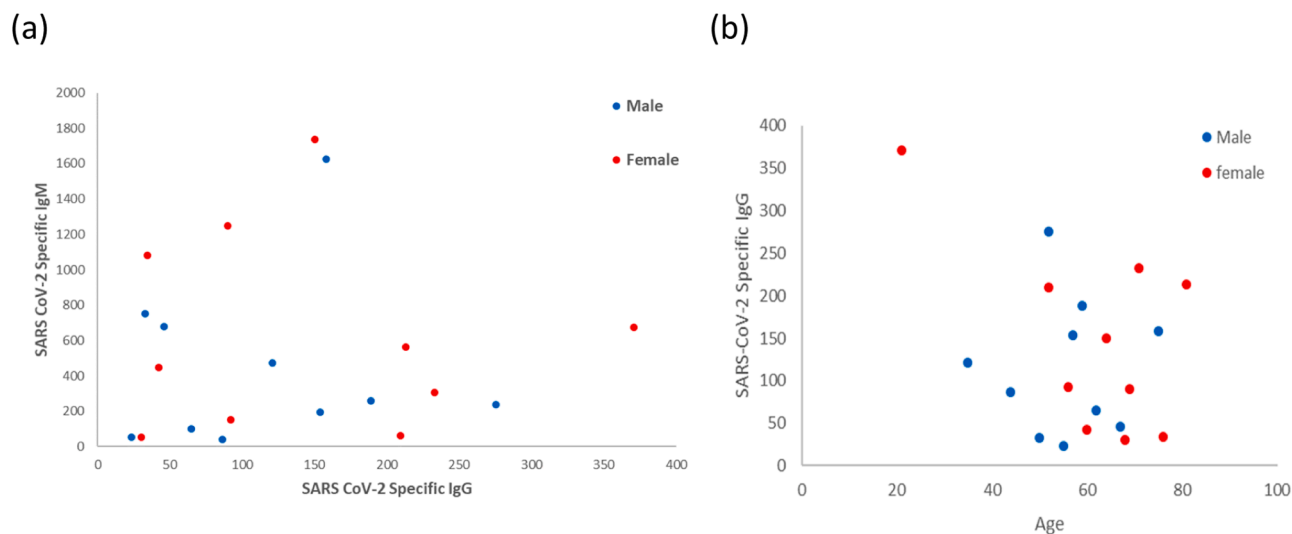


Fig. 1. Analysis of SET A serum samples; (a) SARS CoV-2 Specific IgM versus SARS CoV-2 Specific IgG (Male & Female) (b) SARS CoV-2 Specific IgG versus age.

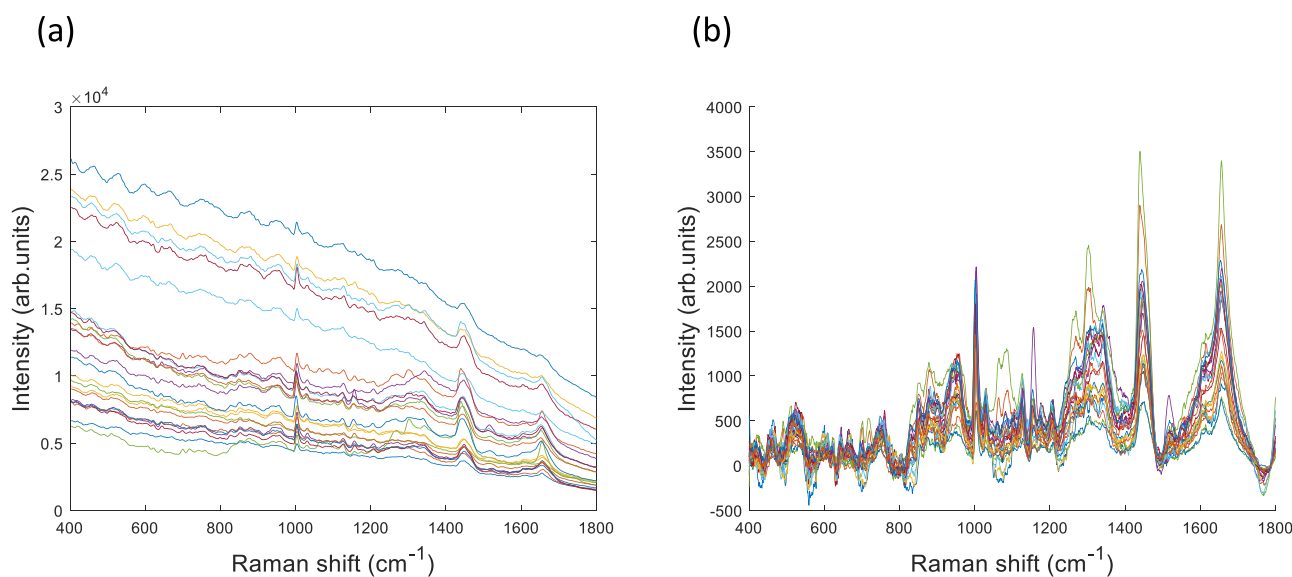


Fig. 2. (a) Raw and (b) preprocessed spectra of COVID-19 positive ( $n = 23$ ) samples.

shown). It is interesting to note, however, that, while the COVID-19 negative group is relatively tightly clustered, a significantly greater variance is observed among the spectra of the COVID-19 positive group. In this context, a similar degree of variance is observed for SET A and SET B samples. In the case of PC1, this variance has origin largely in the protein content, as shown in Fig. 3(c), in which the loading of PC1 is compared to the spectrum of albumin.

### 3.3. Raman spectroscopic analysis of fractionated serum

The intrinsic variance of the Raman spectroscopic response of the serum samples is dominated by that of the high molecular weight proteins, particularly in the case of the COVID-19 positive samples, and may potentially mask pathologically significant variances of lower molecular weight constituents, which can be revealed by fractionating the serum samples for more detailed analysis [34]. As only 5  $\mu\text{L}$  of each SET A and normal sample were available, only SET B was centrifugally fractionated, as described in Section 2.1, and the mean spectra of the respective fractions are compared to similar fractions of human pooled serum, as a negative control, in Fig. 4.

In the case of the 100 kDa (Fig. 4(a)) and 50 kDa (Fig. 4(b)) fractions, there is little or no obvious difference between the spectra of the COVID-19 positive samples and the corresponding fractions of pooled serum. However, marked differences can be seen between the mean spectra of both the 30 kDa and 10 kDa samples, as shown in Fig. 4(c)&(d), and this was further examined by exploring any systematic correlation of the respective 10 kDa and 30 kDa spectra and the SARS-CoV-2 specific IgG antibody levels, for the 5 samples of SET B, as listed in Table 1. Although no clear correlation was observed for the spectra of the 10 kDa samples, PLSR did indicate a correlation of the spectra of the 30 kDa fraction with the COVID-19 specific IgG levels of Table 1.

Fig. 5(a) shows the spectra of the 30 kDa fractions of the 5 SET B samples, which were used to construct a PLSR model, initially with 4 LVs. Based on the percentage variance explained (Fig. 5(b)), the optimum number of Latent Variables was determined to be 2, and the model was reconstructed, producing a linear prediction model of  $R^2 = 1$  (Fig. 5(c)). The PLSR loading plot of the first Latent Variable (Fig. 5(d)) indicates a spectrum which is negatively correlated with increasing IgG levels in the SET B COVID-19 patient serum samples, indicative of a deficiency of one or more constituents in the range 50–30 kDa.



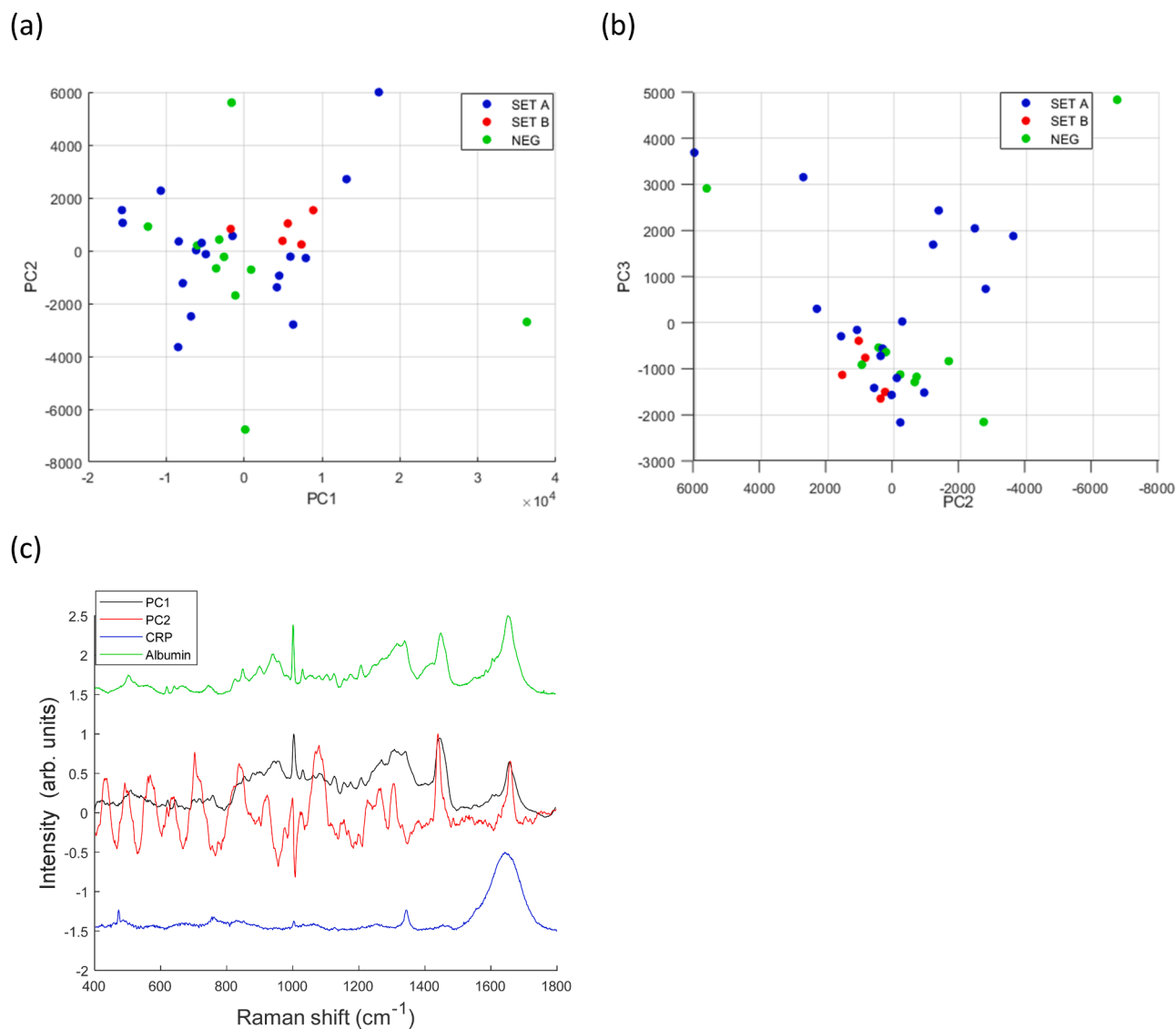


**Fig. 3.** PCA of SARS CoV-2 Specific positive versus SARS CoV-2 negative serum samples. (a) PC2 vs PC1 (b) PC3 vs PC2 (c) Loadings of PC1 (black), PC2 (red) compared to the spectra of Albumin (green) and C-Reactive Protein (blue), both offset.

In Fig. 5(d), a spectrum of glutathione (inverted for ease of comparison) is overlaid on the PLSR Co-efficient. The degree of similarity suggests that glutathione may be a candidate biomarker giving rise to the systematic correlation of the 30 kDa spectral profile with patient IgG levels in the serum of convalescent patients of SET B, consistent with reports associating COVID-19 with a glutathione deficiency [57], meriting further investigation.

#### 4. Discussion and conclusions

The World Health Organisation (WHO) Global Research Roadmap to promote a co-ordinated approach to address the emerging global crisis associated with the COVID pandemic [58] highlighted that there are major gaps in our understanding of many key aspects of the evolution, transmission, and effects of viruses, and emphasised the importance of improved fundamental understanding of the processes associated with viral infection and the development of new tools to monitor viral infection, not just in the context of the SARS-CoV-2 outbreak, but to support responses to other ongoing or future outbreaks across the world. In this context, vibrational spectroscopy has emerged as a potential candidate [59], and in particular, Raman spectroscopy has been

demonstrated as a potential tools for screening human serum, in its liquid form, and fractionated to analyse selected molecular weight ranges [60,61].

To further explore its potential to contribute to the understanding of the effects of COVID-19, this study used Raman spectroscopy to analyse commercially available samples of blood serum of convalescing COVID-19 patients. The available set of serum patient samples were drawn up to 25–37 days (SET A) or 27–134 (SET B) after a positive test for SARS-2-CoV infection. It should be noted, therefore, that this timescale is long compared to the estimated virus replication time ( $\sim 10$  min), and incubation period ( $\sim 5$  days) [62,63]. Antibodies are reportedly detectable in the blood serum 6 days after diagnosis, but begin to fade during convalescence on a varied timescale of weeks to months [4,64]. Nevertheless, the Raman spectroscopic analysis of this study, as a label free bioanalytical technique, sheds light on the variability of the biochemical constitution of the serum samples of the convalescing COVID-19 positive patients.

The meta data from the suppliers provides information on the patient age, sex, time between positive PCR test and blood draw, SARS-CoV-2 specific IgG and IgM levels. As an initial analysis of this meta-data, it is worth noting that:

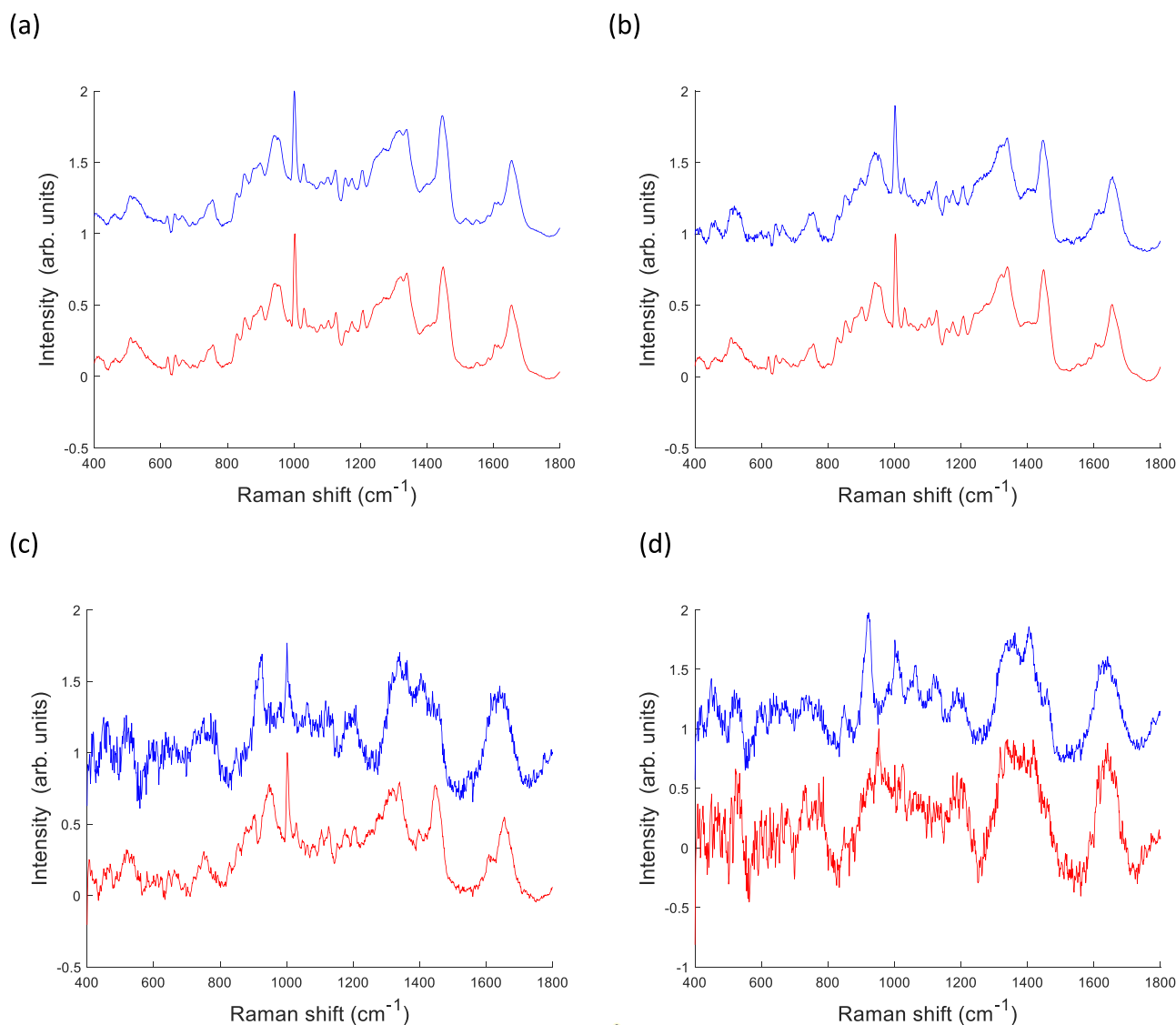


Fig. 4. Comparisons of the mean spectra of COVID-19 positive (blue) and negative (red) serum fractions; (a) 100 kDa, (b) 50 kDa and (c) 30 kDa and (d) 10 kDa.

- There is no correlation between the SARS-CoV-2 specific IgG and IgM levels across the samples.
- There is no differentiation of SARS-CoV-2 specific IgG and IgM levels based on gender, and no obvious correlation with age.

It has been observed that COVID-19 has a relatively long incubation period of about 5–10 days, during which time the infection is detectable by levels of SARS-CoV-2 RNA and antigens [65]. The acute phase of the systemic response begins with early increases in SARS-CoV-2 specific IgM antibodies, peaking within ~ 7–10 days, and this is followed by the manifestation of SARS-CoV-2 specific IgG antibodies, which peak within ~ 2 weeks, but persist beyond 4 weeks after infection, potentially providing long term immunity to the patient. The absence of any quantitative correlation between SARS-CoV-2 specific IgG and IgM levels in the whole serum samples measured ~ 4–5 weeks after a positive test for infection is therefore not unexpected.

Furthermore, based on the Raman spectroscopic analysis:

- COVID-19 negative patients have much lower variance in their spectroscopic profiles (biochemical content) than COVID-19 positive samples

- COVID-19 negative and positive patients are not differentiated by principal components analysis of the Raman spectral signatures.
- The Raman spectroscopic analysis shows no differentiation according to gender, or correlation with age profile
- The primary variance of the Raman spectroscopic response of COVID-19 positive patient samples is due to the high molecular weight protein content.
- The primary variance of the Raman spectroscopic response of patient samples is not correlated with specific IgG or IgM

The metadata of the suppliers indicate that the SARS-CoV-2 specific IgG and IgM levels of the patient samples are elevated by factors as high as 20 and 1000 fold compared to the cut-offs for COVID-19 negative samples, respectively (Table 1). It is important to emphasise, however, that the IgG and IgM levels reported, measured and provided by the supplier (in arbitrary units), relate to IgG and IgM specific for the SARS-CoV-2 spike receptor binding domain. Although the levels of SARS-CoV-2 specific IgM and IgG can vary considerably between patients, as seen in the samples in this study, the quantitative levels are generally in the ng/ml range. However, the total serum levels of IgM and IgG are in the mg/ml range, and are therefore not significantly affected by these specific changes [66]. It may not therefore be surprising that the variations

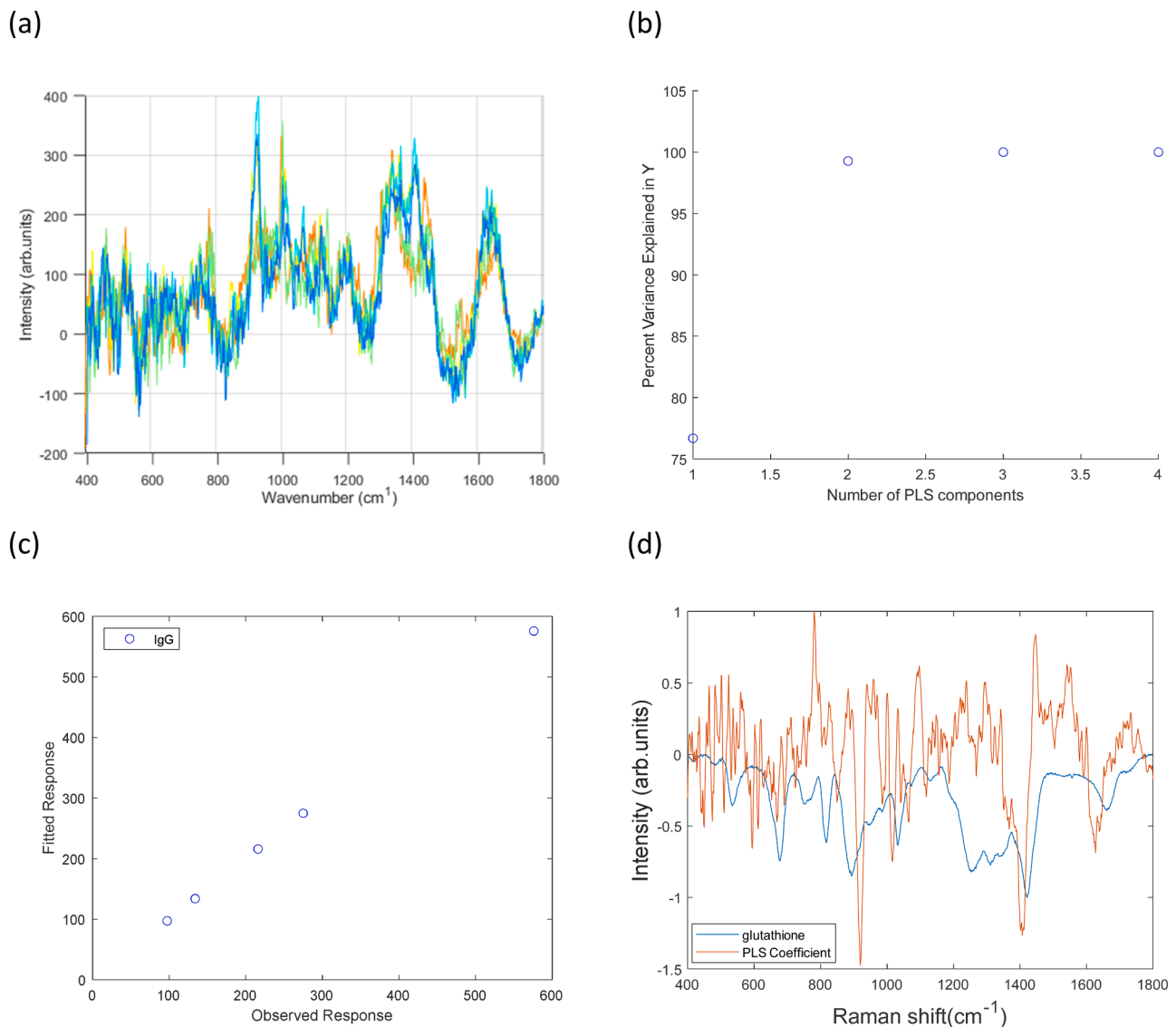


Fig. 5. (a) EMSC corrected Raman spectra of 30 kDa fraction from SET B COVID-19 positive patient serum samples, recorded using the 785 nm laser (b) Cumulative percentage variance explained by the PLS components (c) PLSR prediction model (d) Plot of PLSR loadings.

of the Raman do not correlate with the specific IgG/IgM levels, and that the spectral profile of the PC describing the majority of the variance bears more similarity with that of albumin (Fig. 3(c)), which normally constitutes ~50 % of blood protein. It should be noted that, although no further patient details were made available by the commercial suppliers, additional aspects such as cardio vascular health status, hepatic health status, history of alcoholism are potential confounding factors [67]. Critically, the spectral responses of the two sample sets A and B are not differentiated by PCA, indicating that there is no influence of different collection methods, storage, etc. It is, however, notable that the COVID-19 samples show considerably higher variability in the protein levels than the COVID-19 negative samples. Elevated levels of albumin, hyperalbuminaemia, are commonly associated with acute dehydration [68], whereas decreased levels of albumin, hypoalbuminaemia, are normally associated with, for example, sepsis, liver or kidney disease [69]. In the context of COVID-19, there has been several studies relating higher blood albumin levels in patients with improved prognosis [70], while low levels have been associated with poor prognosis and higher mortality rates [71,72]. Notably, in the study of Kheir et al., 60.2 % of patients were found to be hypoalbuminaemic, rather than hyperalbuminaemic [70]. The samples measured in the current study are of

convalescent patients, which may be consistent with elevated levels of albumin, although it is worth considering other potential protein candidates.

Elevated levels of C reactive protein (CRP) have been reported in some studies [73] and have also been implicated as potential markers of disease severity [74,75]. It is noted, however, that the spectral profile of the loading of the first PC of the comparison of SET A COVID 19 positive and negative samples does not match well that of CRP (Fig. 3(c)). Although the monomer unit of CRP has a molecular mass of ~25 kDa, in serum it is present as a pentameric structure of molecular mass ~120 kDa [76]. There is no specific evidence of elevated levels of CRP in the spectrum of the > 100 kDa fraction of SET B, shown in Fig. 4(a), however. Amongst the established clinical features of COVID-19 are thromboinflammation and coagulopathy, associated with acute pulmonary injury and inflammation [77,78]. COVID-19 has been associated with increased levels of coagulant factors such as thrombin [79], which could also contribute to increased levels of serum protein content, as identified by the Raman spectroscopic analysis, and may play an important role in both acute COVID-19 infection as well as the chronic problems affecting a subset of infected individuals [80].

The large variance of the high molecular weight protein content of



the COVID-19 positive serum samples potentially mask underlying variances of low molecular weight components which may potentially be more valuable in the context of longitudinal studies, disease prognosis and therapeutic intervention, for example with the different forms of vaccines. Fractionation, particularly by centrifugal filtration, is a technique commonly used in proteomics [81–83], and has been previously used in the IR [84,85] and Raman [42,86] analysis of human serum. In the case of Raman analysis, analysis of the concentrated fraction has been shown to be particularly advantageous as it provides enhanced signals, which retain the relative concentrations of constituent components, enabling quantitative analysis of clinically relevant high and low molecular biomolecules in blood such as immunoglobulins, albumin, glucose and urea [35,60,87], as well as saliva [88]. COVID-19 has, in particular, been associated with depleted levels of the antioxidant glutathione (GSH), due to increased oxidative stress [89]. GSH is synthesised in cells, particularly in the liver, and low levels have been associated with a range of chronic conditions [90–92], multimorbidity [93] and aging [94]. Glutathione deficiency has previously been associated with viral infection [95], and was quickly identified as a symptom of adults hospitalised with COVID-19 [96]. Similarly, oxidative stress as a result of excessive production of reactive oxygen species (ROS) has been reported to be associated with high COVID-19 mortality [97]. Glutathione has been observed to play a role in prevention of COVID-19 immunothrombosis [98], and glutathione supplementation has been proposed as an adjunct therapy for treatment of COVID-19 patients [95, 99]. Furthermore, oxidative damage and diminished antioxidant levels have been identified amongst the extended symptoms of COVID-19, indicating that glutathione deficiency may be an important clinical factor in monitoring patient recovery [100].

The spectral profile of the PLSR of the 30 kDa fraction of the SET B convalescing COVID-19 patients bears a striking resemblance to the spectrum of glutathione. Notably, the Raman spectrum of glutathione has been shown to be highly dependent on pH and concentration [101], and thus an inexact match to the spectral signature of a deficiency in the complex medium of human serum may not be surprising. In blood, glutathione binds to proteins through S-glutathionylation [102–104], to protect the thiol groups of proteins against over-oxidation to sulfonic acid [105], and S-glutathionylated proteins (PSSG) are considered to be reliable biomarkers of oxidative stress [106]. Although albumin is the most abundant thiol containing serum protein [107], a number of studies have indicated important roles of S-glutathionylation of lower molecular weight serum proteins, in, for example, carotid artery stenosis [108], arteriosclerosis [109] and more generally in cardiac disorders, therapies, and diagnosis [110]. While such studies indicate elevated levels of PSSGs as diagnostic indicators, the negative correlation of the PLSR analysis of the 30 kDa fraction may be indicative of reduced levels of PSSGs in the range 50–30 kDa in convalescing COVID-19 patients, due to the reduced levels of GSH, correlated with COVID-19 specific IgG levels, as an indication of disease severity.

Therefore, although the analysis of the whole serum samples of convalescent COVID-19 patients did not yield anything of immediately evident value, the study has demonstrated the potential of Raman spectroscopy as an analytical tool to monitor and potentially further the understanding of the manifestation of persistent biomarkers of disease in convalescent patients. Further studies are required on larger cohorts, also potentially including vaccinated and “long COVID” sufferers, to confirm and elaborate our findings.

#### Declaration of Competing Interest

The authors declares that there is no conflict of interest for the study “Raman Spectroscopic analysis of human serum samples of convalescing COVID-19 positive patients.”

#### Data Availability

Data will be made available on request.

#### References

- [1] M. Ciotti, M. Ciccozzi, A. Terrinoni, W.C. Jiang, C. Bin Wang, S. Bernardini, The COVID-19 pandemic, *Crit. Rev. Clin. Lab Sci.* 57 (6) (2020) 365–388 (Available from), (<https://www.tandfonline.com/doi/abs/10.1080/10408363.2020.1783198>) [cited 2023 Apr 29].
- [2] M. Buheji, K. da Costa Cunha, G. Beka, B. Mavrić, Y. Leandro do Carmo de Souza, S. Souza da Costa Silva, et al., The extent of COVID-19 pandemic socio-economic impact on global poverty. A global integrative multidisciplinary review, *Am. J. Econ.* 10 (4) (2020) 213–224.
- [3] World Health Organization. A coordinated Global Research Roadmap to respond to the D-19 epidemic and beyond. R&DBLueprint. 2020.
- [4] P.G. Choe, K.H. Kim, C.K. Kang, H.J. Suh, E.K. Kang, S.Y. Lee, et al., Antibody responses 8 months after asymptomatic or mild SARS-CoV-2 infection, *Emerg. Infect. Dis.* 27 (3) (2021) 928–931.
- [5] N.M. Ralbovsky, I.K. Lednev, Towards development of a novel universal medical diagnostic method: Raman spectroscopy and machine learning, *Chem. Soc. Rev.* (2020) 7428–7453.
- [6] M.J. Baker, H.J. Byrne, J. Chalmers, P. Gardner, R. Goodacre, A. Henderson, et al., Clinical applications of infrared and Raman spectroscopy: State of play and future challenges, *Analyst* 143 (8) (2018) 1735–1757.
- [7] H.J. Byrne, M. Baranska, G.J. Puppels, N. Stone, B. Wood, K.M. Gough, et al., Spectroscopy for the next generation: Quo vadis? *Analyst* 140 (7) (2015) 2066–2073.
- [8] K. Naseer, S. Ali, J. Qazi, ATR-FTIR spectroscopy as the future of diagnostics: a systematic review of the approach using bio-fluids, *Appl. Spectrosc. Rev.* (2020) 1–13, <https://doi.org/10.1080/05704928.2020.1738453>.
- [9] E. Barnas, J. Skret-Magierlo, A. Skret, E. Kaznowska, J. Depciuch, K. Szumc, et al., Simultaneous FTIR and Raman spectroscopy in endometrial atypical hyperplasia and cancer, *Int. J. Mol. Sci.* 21 (14) (2020) 1–13.
- [10] S. Roy, D. Perez-Guaita, S. Bowden, P. Heraud, B.R. Wood, Spectroscopy goes viral: diagnosis of hepatitis B and C virus infection from human sera using ATR-FTIR spectroscopy, *Clin. Spectrosc.* 1 (October 2019) (2019), 100001, <https://doi.org/10.1016/j.clispe.2020.100001>.
- [11] M. Sbroscia, M. di Gioacchino, P. Ascenzi, P. Crucitti, A. di Masi, I. Giovannoni, et al., Thyroid cancer diagnosis by Raman spectroscopy, *Sci. Rep.* 10 (1) (2020) 1–10, <https://doi.org/10.1038/s41598-020-70165-0>.
- [12] G. Calado, I. Behl, H.J. Byrne, F.M. Lyng, Raman spectroscopic characterisation of non stimulated and stimulated human whole saliva, *Clin. Spectrosc.* 3 (2021), 100010.
- [13] H.J. Byrne, F. Bonnier, J. McIntyre, D.R. Parachalil, Quantitative analysis of human blood serum using vibrational spectroscopy, *Clin. Spectrosc.* 2 (2020), 100004.
- [14] J. Saade, M.T.T. Pacheco, M.R. Rodrigues, L. Silveira, Identification of hepatitis C in human blood serum by near-infrared Raman spectroscopy, *Spectroscopy* 22 (5) (2008) 387–395.
- [15] D.R. Parachalil, J. McIntyre, H.J. Byrne, Potential of Raman spectroscopy for the analysis of plasma/serum in the liquid state: recent advances, *Anal. Bioanal. Chem.* 412 (9) (2020) 1993–2007.
- [16] C. Chen, J. Wang, C. Chen, J. Tang, X. Lv, C. Ma, Rapid and efficient screening of human papillomavirus by Raman spectroscopy based on GA-SVM, *Optik (Stuttg)* 210 (March) (2020), 164514, <https://doi.org/10.1016/j.ijleo.2020.164514>.
- [17] X. Wang, S. Tian, L. Yu, X. Lv, Z. Zhang, Rapid screening of hepatitis B using Raman spectroscopy and long short-term memory neural network, *Lasers Med. Sci.* 35 (8) (2020) 1791–1799.
- [18] K.M. Ostrowska, A. Malkin, A. Meade, J. O’Leary, C. Martin, C. Spillane, et al., Investigation of the influence of high-risk human papillomavirus on the biochemical composition of cervical cancer cells using vibrational spectroscopy, *Analyst* 135 (12) (2010) 3087–3093.
- [19] L.G. Silva, A.F.S. Péres, D.L.D. Freitas, C.L.M. Morais, F.L. Martin, J.C.O. Crispim, et al., ATR-FTIR spectroscopy in blood plasma combined with multivariate analysis to detect HIV infection in pregnant women, *Sci. Rep.* 10 (1) (2020) 1–7, <https://doi.org/10.1038/s41598-020-77378-3>.
- [20] A. Ditta, H. Nawaz, T. Mahmood, M.I. Majeed, M. Tahir, N. Rashid, et al., Principal components analysis of Raman spectral data for screening of Hepatitis C infection, *Spectrochim. Acta A Mol. Biomol. Spectrosc.* 221 (2019), 117173, <https://doi.org/10.1016/j.saa.2019.117173>.
- [21] T. Mahmood, H. Nawaz, A. Ditta, M.I. Majeed, M.A. Hanif, N. Rashid, et al., Raman spectral analysis for rapid screening of dengue infection, *Spectrochim. Acta A Mol. Biomol. Spectrosc.* 200 (2018) 136–142, <https://doi.org/10.1016/j.saa.2018.04.018>.
- [22] H. Nawaz, N. Rashid, M. Saleem, M. Asif Hanif, M. Irfan Majeed, I. Amin, et al., Prediction of viral loads for diagnosis of hepatitis C infection in human plasma samples using Raman spectroscopy coupled with partial least squares regression analysis, *J. Raman Spectrosc.* 48 (5) (2017) 697–704.
- [23] L.F. Carvalho, C. e S. das, M.S. de, Nogueira, Optical techniques for fast screening – towards prevention of the coronavirus COVID-19 outbreak, *Photo Photo Ther.* 30 (2020), 101765.
- [24] D. Graham, Can Raman spectroscopy be a useful tool in the fight against COVID-19? *Spectrosc. (St. Monica)* 35 (6) (2020) 44–46.

- [25] R.S. Khan, I.U. Rehman, Spectroscopy as a tool for detection and monitoring of Coronavirus (COVID-19), *Expert Rev. Mol. Diagn.* 20 (7) (2020) 647–649.
- [26] J. Lukose, S. Chidangil, S.D. George, Optical technologies for the detection of viruses like COVID-19: progress and prospects, *Biosens. Bioelectron.* 178 (2021), 113004.
- [27] A.C.C. Goulart, L. Silveira, H.C. Carvalho, C.B. Dorta, M.T.T. Pacheco, R. A. Zângaro, Diagnosing COVID-19 in human serum using Raman spectroscopy, *Lasers Med. Sci.* 37 (4) (2022) 2217–2226, <https://doi.org/10.1007/s10103-021-03488-7>.
- [28] A. Bedair, K. Okasha, F.R. Mansour, Spectroscopic methods for COVID-19 detection and early diagnosis, *Virology* 19 (1) (2022) 1–13, <https://doi.org/10.1186/s12985-022-01867-2>.
- [29] D.L. Kitane, S. Loukman, N. Marchoudi, A. Fernandez-Galiana, F.Z. el Ansari, F. Jouali, et al., A simple and fast spectroscopy-based technique for Covid-19 diagnosis, *Sci. Rep.* 11 (1) (2021) 1–11, <https://doi.org/10.1038/s41598-021-95568-5>.
- [30] D. Zhang, X. Zhang, R. Ma, S. Deng, X. Wang, X. Zhang, et al., Ultra-fast and onsite interrogation of severe acute respiratory syndrome coronavirus 2 (SARS-CoV-2) in environmental specimens via surface enhanced Raman scattering (SERS), *Water Res.* (2020). May;2020.05.02.20086876.
- [31] V.G. Barauna, M.N. Singh, L.L. Barbosa, W.D. Marcarini, P.F. Vassallo, J.G. Mill, et al., Ultrarapid on-site detection of SARS-CoV-2 infection using simple ATR-FTIR spectroscopy and an analysis algorithm: high sensitivity and specificity, *Anal. Chem.* 93 (5) (2021) 2950–2958.
- [32] B.R. Wood, K. Kochan, D.E. Bedolla, N. Salazar-Quiroz, S.L. Grimley, D. Perez-Guaita, et al., Infrared based saliva screening test for COVID-19, *Angew. Chem.* 133 (31) (2021) 17239–17244.
- [33] V.G. Barauna, M.N. Singh, L.L. Barbosa, W.D. Marcarini, P.F. Vassallo, J.G. Mill, et al., Ultrarapid on-site detection of SARS-CoV-2 infection using simple ATR-FTIR spectroscopy and an analysis algorithm: high sensitivity and specificity, *Anal. Chem.* 93 (5) (2021) 2950–2958.
- [34] F. Bonnier, F. Petitjean, M.J. Baker, H.J. Byrne, Improved protocols for vibrational spectroscopic analysis of body fluids, *J. Biophotonics* 7 (3–4) (2014) 167–179.
- [35] D.R. Parachalil, C. Bruno, F. Bonnier, H. Blasco, I. Chourpa, M.J. Baker, et al., Analysis of bodily fluids using vibrational spectroscopy: a direct comparison of Raman scattering and infrared absorption techniques for the case of glucose in blood serum, *Analyst* 144 (10) (2019) 3334–3346.
- [36] P.C. Matthews, M.I. Andersson, C.V. Arancibia-Carcamo, K. Auckland, J. K. Baillie, E. Barnes, et al., SARS-CoV-2 RNA detected in blood products from patients with COVID-19 is not associated with infectious virus, *Wellcome Open Res.* (2020) 5. (<https://pubmed.ncbi.nlm.nih.gov/33283055/>).
- [37] P.G. Choe, K.H. Kim, C.K. Kang, H.J. Suh, E.K. Kang, S.Y. Lee, et al., Antibody responses 8 months after asymptomatic or mild SARS-CoV-2 infection, *Emerg. Infect. Dis.* 27 (3) (2021) 928–931.
- [38] G.E. Hartley, E.S.J. Edwards, P.M. Aui, N. Varese, S. Stojanovic, J. McMahon, et al., Rapid generation of durable B cell memory to SARS-CoV-2 spike and nucleocapsid proteins in COVID-19 and convalescence, *Sci. Immunol.* 5 (54) (2020).
- [39] G. Yin, L. Li, S. Lu, Y. Yin, Y. Su, Y. Zeng, et al., An efficient primary screening of COVID-19 by serum Raman spectroscopy, *J. Raman Spectrosc.* 52 (5) (2021) 949–958.
- [40] N.A. Pinsky, J.M. Huddleston, R.M. Jacobson, P.C. Wollan, G.A. Poland, Effect of multiple freeze-thaw cycles on detection of measles, mumps, and rubella virus antibodies, *Clin. Diagn. Lab Immunol.* 10 (1) (2003) 19–21.
- [41] A. Torelli, E. Giancetti, M. Monti, P. Piu, I. Barneschi, C. Bonifazi, et al., Effect of repeated freeze-thaw cycles on influenza virus antibodies, *Vaccin. (Basel)* 9 (3) (2021) 267.
- [42] F. Bonnier, M.J. Baker, H.J. Byrne, Vibrational spectroscopic analysis of body fluids: avoiding molecular contamination using centrifugal filtration, *Analytical, Methods* 6 (14) (2014) 5155–5160.
- [43] F. Bonnier, F. Petitjean, M.J. Baker, H.J. Byrne, Improved protocols for vibrational spectroscopic analysis of body fluids, *J. Biophotonics* 7 (3–4) (2014) 167–179.
- [44] D.R. Parachalil, Screening of human serum/plasma using vibrational spectroscopy for early disease diagnostics and therapeutic drug monitoring, *Technol. Univ. Dublin* (2019).
- [45] D.R. Parachalil, J. McIntyre, H.J. Byrne, Potential of Raman spectroscopy for the analysis of plasma/serum in the liquid state: recent advances, *Anal. Bioanal. Chem.* 412 (9) (2020) 1993–2007.
- [46] H.J. Byrne, P. Knief, M.E. Keating, F. Bonnier, Spectral pre and post processing for infrared and Raman spectroscopy of biological tissues and cells, *Chem. Soc. Rev.* 45 (7) (2016) 1865–1878.
- [47] L.T. Kerr, B.M. Hennelly, A multivariate statistical investigation of background subtraction algorithms for Raman spectra of cytology samples recorded on glass slides, *Chemom. Intell. Lab. Syst.* 158 (August) (2016) 61–68.
- [48] F. Bonnier, A. Mehmood, P. Knief, A.D. Meade, W. Hornebeck, H. Lambkin, et al., In vitro analysis of immersed human tissues by Raman microspectroscopy, *J. Raman Spectrosc.* 42 (5) (2011) 888–896.
- [49] D.R. Parachalil, B. Brankin, J. McIntyre, H.J. Byrne, Raman spectroscopic analysis of high molecular weight proteins in solution-considerations for sample analysis and data pre-processing, *Analyst* 143 (24) (2018) 5987–5998.
- [50] L.T. Kerr, B.M. Hennelly, A multivariate statistical investigation of background subtraction algorithms for Raman spectra of cytology samples recorded on glass slides, *Chemom. Intell. Lab. Syst.* 158 (August) (2016) 61–68.
- [51] F. Bonnier, H.J. Byrne, Understanding the molecular information contained in principal component analysis of vibrational spectra of biological systems, *Analyst* 137 (2) (2012) 322–332.
- [52] J.M. Cameron, C. Bruno, D.R. Parachalil, M.J. Baker, F. Bonnier, H.J. Butler, et al., Vibrational spectroscopic analysis and quantification of proteins in human blood plasma and serum. *Vibrational Spectroscopy in Protein Research*, Elsevier, 2020, pp. 269–314.
- [53] D.R. Parachalil, C. Bruno, F. Bonnier, H. Blasco, I. Chourpa, J. McIntyre, et al., Raman spectroscopic screening of high and low molecular weight fractions of human serum, *Analyst* 144 (14) (2019) 4295–4311.
- [54] J. Udensi, E. Loskutova, J. Loughman, H.J. Byrne, Quantitative Raman analysis of carotenoid protein complexes in aqueous solution, *Molecules* 27 (15) (2022).
- [55] F. Bonnier, A. Mehmood, P. Knief, A.D. Meade, W. Hornebeck, H. Lambkin, et al., In vitro analysis of immersed human tissues by Raman microspectroscopy, *J. Raman Spectrosc.* 42 (5) (2011) 888–896.
- [56] D.R. Parachalil, J. McIntyre, H.J. Byrne, Potential of Raman spectroscopy for the analysis of plasma/serum in the liquid state: recent advances, *Anal. Bioanal. Chem.* 412 (9) (2020) 1993–2007.
- [57] Shell A cruce. Baylor College of Medicine. 2021 [cited 2023 Mar 21]. p. 1–23 COVID-19 patients have increased oxidative stress, oxidant damage, and glutathione deficiency. Available from: (<https://www.bcm.edu/news/covid-19-patients-have-increased-oxidative-stress-oxidant-damage-and-glutathione-deficiency>).
- [58] World Health Organization. A coordinated Global Research Roadmap to respond to the-19 epidemic and beyond. R&DBlueprint. 2020.
- [59] Chaudhary I., Jackson N., Denning D., O'Neill L., Byrne H.J. Contributions of vibrational spectroscopy to virology: a review. *Clinical Spectroscopy* [Internet]. 2022 Dec [cited 2022 Nov 9];4:100022. Available from: /pmc/articles/PMC9093054/.
- [60] H.J. Byrne, F. Bonnier, J. McIntyre, D.R. Parachalil, Quantitative analysis of human blood serum using vibrational spectroscopy, *Clin. Spectrosc.* 2 (2020), 100004.
- [61] D.R. Parachalil, J. McIntyre, H.J. Byrne, Potential of Raman spectroscopy for the analysis of plasma/serum in the liquid state: recent advances, *Anal. Bioanal. Chem.* 412 (9) (2020) 1993–2007.
- [62] J.H. Choe, Two weeks, *Ann. Intern. Med.* 172 (10) (2020) 697–698.
- [63] Y.M. Bar-On, A. Flamholz, R. Phillips, R. Milo, Sars-cov-2 (Covid-19) by the numbers, *Elife* (2020) 9.
- [64] G.E. Hartley, E.S.J. Edwards, P.M. Aui, N. Varese, S. Stojanovic, J. McMahon, et al., Rapid generation of durable B cell memory to SARS-CoV-2 spike and nucleocapsid proteins in COVID-19 and convalescence, *Sci. Immunol.* 5 (54) (2020) 1–14.
- [65] A.K. Azkur, M. Akdis, D. Azkur, M. Sokolowska, W. van de Veen, M.C. Brügggen, et al., Immune response to SARS-CoV-2 and mechanisms of immunopathological changes in COVID-19, *Allergy: Eur. J. Allergy Clin. Immunol.* 75 (7) (2020) 1564–1581.
- [66] E. Marklund, S. Leach, H. Axelsson, K. Nyström, H. Norder, M. Bemark, et al., Erratum: Serum-IgG responses to SARS-CoV-2 after mild and severe COVID-19 infection and analysis of IgG non-responders, in: *PLoS One*, 15, 2020, p. 10, <https://doi.org/10.1371/journal.pone.0241104>.
- [67] M. Diem, Comments on recent reports on infrared spectral detection of disease markers in blood components, in: *J. Biophotonics*, 11, 2018, e201800064 (Available from), (<https://onlinelibrary.wiley.com/doi/full/10.1002/jbio.201800064>).
- [68] Busher J.T. Serum Albumin and Globulin. *Clinical Methods: The History, Physical, and Laboratory Examinations* [Internet]. 1990; Available from: (<http://www.ncbi.nlm.nih.gov/pubmed/21250048>).
- [69] M.E. Jellings, D.P. Henriksen, P. Hallas, M. Brabrand, Hypoalbuminemia is a strong predictor of 30-day all-cause mortality in acutely admitted medical patients: a prospective, observational, cohort study, *PLoS One* 9 (8) (2014) 8–12.
- [70] M. Kheir, F. Saleem, C. Wang, A. Mann, J. Chua, Higher albumin levels on admission predict better prognosis in patients with confirmed COVID-19, *PLoS One* 16 (3 March) (2021) 1–10, <https://doi.org/10.1371/journal.pone.0248358>.
- [71] F. Violi, R. Cangemi, G.F. Romiti, G. Ceccarelli, A. Oliva, F. Alessandri, et al., Is albumin predictor of mortality in COVID-19? *Antioxid. Redox Signal* 35 (2) (2021) 139–142.
- [72] P. Paliogiannis, A.A. Mangoni, M. Cangemi, A.G. Fois, C. Carru, A. Zinellu, Serum albumin concentrations are associated with disease severity and outcomes in coronavirus 19 disease (COVID-19): a systematic review and meta-analysis, *Clin. Exp. Med.* 21 (3) (2021) 343–354, <https://doi.org/10.1007/s10238-021-00686-z>.
- [73] P. Paliogiannis, A.A. Mangoni, M. Cangemi, A.G. Fois, C. Carru, A. Zinellu, Serum albumin concentrations are associated with disease severity and outcomes in coronavirus 19 disease (COVID-19): a systematic review and meta-analysis, *Clin. Exp. Med.* 21 (3) (2021) 343–354.
- [74] C. Tan, Y. Huang, F. Shi, K. Tan, Q. Ma, Y. Chen, et al., C-reactive protein correlates with computed tomographic findings and predicts severe COVID-19 early, *J. Med. Virol.* 92 (7) (2020) 856–862.
- [75] N. Ali, Elevated level of C-reactive protein may be an early marker to predict risk for severity of COVID-19, *J. Med. Virol.* 92 (11) (2020) 2409–2411.
- [76] D. Thompson, M.B. Pepys, S.P. Wood, The physiological structure of human C-reactive protein and its complex with phosphocholine, *Structure* 7 (2) (1999) 169–177. Feb 15.
- [77] W.B. Mitchell, Thromboinflammation in COVID-19 acute lung injury, *Paediatr. Respir. Rev.* 35 (2020) 20–24, <https://doi.org/10.1016/j.prrv.2020.06.004>.

- [78] K. Sriram, P.A. Insel, Inflammation and thrombosis in covid-19 pathophysiology: proteinase-activated and purinergic receptors as drivers and candidate therapeutic targets, *Physiol. Rev.* 101 (2) (2021) 545–567.
- [79] E.G. Bouck, F. Denorme, L.A. Holle, E.A. Middleton, A.M. Blair, B. De Laet, et al., COVID-19 and Sepsis Are Associated with Different Abnormalities in Plasma Procoagulant and Fibrinolytic Activity, *Arterioscler. Thromb. Vasc. Biol.* 41 (1) (2021) 401–414.
- [80] S.E. Lind, Phosphatidylserine is an overlooked mediator of COVID-19 thromboinflammation, *Heliyon* 7 (1) (2021).
- [81] I. Finoulst, M. Pinkse, W. Van Dongen, P. Verhaert, Sample preparation techniques for the untargeted LC-MS-based discovery of peptides in complex biological matrices, *J. Biomed. Biotechnol.* (2011) 2011.
- [82] S. Roche, A. Gabelle, S. Lehmann, Clinical proteomics of the cerebrospinal fluid: towards the discovery of new biomarkers, in: *Proteomics Clin Appl*, 2, 2008, pp. 428–436. (<https://onlinelibrary.wiley.com/doi/full/10.1002/prca.200780040>).
- [83] K. Merrell, K. Southwick, S.W. Graves, M. Sean Esplin, N.E. Lewis, C.D. Thulin, Analysis of low-abundance, low-molecular-weight serum proteins using mass spectrometry, *J. Biomol. Tech.* 15 (4) (2004) 238–248. Available from: [/pmc/articles/PMC2291707/](https://pubmed.ncbi.nlm.nih.gov/161707/).
- [84] J.R. Hands, P. Abel, K. Ashton, T. Dawson, C. Davis, R.W. Lea, et al., Investigating the rapid diagnosis of gliomas from serum samples using infrared spectroscopy and cytokine and angiogenesis factors, *Anal. Bioanal. Chem.* 405 (23) (2013) 7347–7355.
- [85] J.R. Hands, K.M. Dorling, P. Abel, K.M. Ashton, A. Brodbelt, C. Davis, et al., Attenuated total reflection fourier transform infrared (ATR-FTIR) spectral discrimination of brain tumour severity from serum samples, *J. Biophoton.* 7 (3–4) (2014) 189–199.
- [86] F. Bonnier, F. Petitjean, M.J. Baker, H.J. Byrne, Improved protocols for vibrational spectroscopic analysis of body fluids, *J. Biophotonics* 7 (3–4) (2014) 167–179.
- [87] D.R. Parachalil, C. Bruno, F. Bonnier, H. Blasco, I. Chourpa, J. McIntyre, et al., Raman spectroscopic screening of high and low molecular weight fractions of human serum, *Analyst* 144 (14) (2019) 4295–4311.
- [88] G. Calado, I. Behl, H.J. Byrne, F.M. Lyng, Raman spectroscopic characterisation of non stimulated and stimulated human whole saliva, *Clin. Spectrosc.* 3 (2021), 100010.
- [89] P. Kumar, O. Osahon, D.B. Vides, N. Hanania, C.G. Minard, R.V. Sekhar, Severe glutathione deficiency, oxidative stress and oxidant damage in adults hospitalized with covid-19: Implications for glynac (glycine and n-acetylcysteine) supplementation, *Antioxidants* 11 (1) (2022).
- [90] K. Murakami, K. Takahito, Y. Ohtsuka, Y. Fujiwara, M. Shimada, Y. Kawakami, Impairment of glutathione metabolism in erythrocytes from patients with diabetes mellitus, *Metabolism* 38 (8) (1989) 753–758.
- [91] G. Wu, Y.Z. Fang, S. Yang, J.R. Lupton, N.D. Turner, Glutathione metabolism and its implications for health, *J. Nutr.* 134 (3) (2004) 489–492. Mar 1.
- [92] R. Franco, O.J. Schoneveld, A. Pappa, M.I. Panayiotidis, The central role of glutathione in the pathophysiology of human diseases, *Arch. Physiol. Biochem* 113 (4–5) (2007) 234–258. (<https://www.tandfonline.com/doi/abs/10.1080/13813450701661198>).
- [93] L.M. Pérez, B. Hooshmand, F. Mangialasche, P. Mecocci, A.D. Smith, H. Refsum, et al., Glutathione serum levels and rate of multimorbidity development in older adults, *J. Gerontol. - Ser. A Biol. Sci. Med. Sci.* 75 (6) (2020) 1089–1094 (Available from), (<https://academic.oup.com/biomedgerontology/article/75/6/1089/5479550>).
- [94] P.S. Samiec, C. Drews-Botsch, E.W. Flagg, J.C. Kurtz, P. Sternberg, R.L. Reed, et al., Glutathione in human plasma: Decline in association with aging, age-related macular degeneration, and diabetes, *Free Radic. Biol. Med.* 24 (5) (1998) 699–704. Mar 15.
- [95] V. Guloyan, B. Oganessian, N. Baghdasaryan, C. Yeh, M. Singh, F. Guilford, et al., Glutathione supplementation as an adjunctive therapy in COVID-19, *Antioxidants* 9 (2020) 1–22. ([www.mdpi.com/journal/antioxidants](http://www.mdpi.com/journal/antioxidants)).
- [96] P. Kumar, O. Osahon, D.B. Vides, N. Hanania, C.G. Minard, R.V. Sekhar, Severe glutathione deficiency, oxidative stress and oxidant damage in adults hospitalized with covid-19: Implications for glynac (glycine and n-acetylcysteine) supplementation, *Antioxidants* 11 (1) (2022). (<https://pubmed.ncbi.nlm.nih.gov/35052554/>).
- [97] C.A. Labarrere, G.S. Kassab, Glutathione deficiency in the pathogenesis of SARS-CoV-2 infection and its effects upon the host immune response in severe COVID-19 disease, *Front Microbiol.* 13 (October) (2022) 1–25.
- [98] I. Glassman, N. Le, M. Mirhosseini, C.A. Alcantara, A. Asif, A. Goulding, et al., The role of glutathione in prevention of COVID-19 immunothrombosis: a review, *Front Biosci.* 28 (3) (2023) 59 (Available from), (<https://pubmed.ncbi.nlm.nih.gov/37005767/>).
- [99] Lana J.F.S.D., Lana A.V.S.D., Rodrigues Q.S., Santos G.S., Navani R., Navani A., et al. Nebulization of glutathione and N-Acetylcysteine as an adjuvant therapy for COVID-19 onset. *Advances in Redox Research* [Internet]. 2021 Dec [cited 2023 Apr 29];3:100015. Available from: [/pmc/articles/PMC8349474/](https://pubmed.ncbi.nlm.nih.gov/37005767/).
- [100] H.K. Al-Hakeim, H.T. Al-Rubaye, D.S. Al-Hadrawi, A.F. Almula, M. Maes, Long-COVID post-viral chronic fatigue and affective symptoms are associated with oxidative damage, lowered antioxidant defenses and inflammation: a proof of concept and mechanism study, *Mol. Psychiatry* 28 (2) (2023) 564–578 (Available from), (<https://www.nature.com/articles/s41380-022-01836-9>). Oct 24 [cited 2023 Apr 7].
- [101] S. Catalini, B. Rossi, P. Foggi, C. Masciovecchio, F. Bruni, Aqueous solvation of glutathione probed by UV resonance Raman spectroscopy, *J. Mol. Liq.* 283 (2019) 537–547, (<https://doi.org/10.1016/j.molliq.2019.03.113>).
- [102] B.J. Mills, C.A. Lang, Differential distribution of free and bound glutathione and cyst(e)ine in human blood, *Biochem. Pharm.* 52 (3) (1996) 401–406 (Available from), (<https://pubmed.ncbi.nlm.nih.gov/8687493/>).
- [103] E.Y. Park, N. Shimura, T. Konishi, Y. Sauchi, S. Wada, W. Aoi, et al., Increase in the protein-bound form of glutathione in human blood after the oral administration of glutathione, *J. Agric. Food Chem.* 62 (26) (2014) 6183–6189. (<https://pubmed.ncbi.nlm.nih.gov/24877771/>).
- [104] T. Duysak, A.R. Afzal, C.H. Jung, Determination of glutathione-binding to proteins by fluorescence spectroscopy, *Biochem. Biophys. Res Commun.* 557 (2021) 329–333 (Available from), (<https://pubmed.ncbi.nlm.nih.gov/33895474/>).
- [105] C.H. Jung, J.A. Thomas, S-glutathionylated hepatocyte proteins and insulin disulfides as substrates for reduction by glutaredoxin, thioredoxin, protein disulfide isomerase, and glutathione, *Arch. Biochem. Biophys.* 335 (1) (1996) 61–72. (<https://pubmed.ncbi.nlm.nih.gov/8914835/>).
- [106] R. Rossi, I. Dalle-Donne, A. Milzani, D. Giustarini, Oxidized forms of glutathione in peripheral blood as biomarkers of oxidative stress, *Clin. Chem.* 52 (7) (2006) 1406–1414. (<https://pubmed.ncbi.nlm.nih.gov/16690733/>).
- [107] L. Turell, R. Radi, B. Alvarez, The thiol pool in human plasma: the central contribution of albumin to redox processes, *Free Radic. Biol. Med.* 65 (2013) 244–253.
- [108] M. Nakamoto, M. Hirose, M. Kawakatsu, T. Nakayama, Y. Urata, K. Kamata, et al., Serum S-glutathionylated proteins as a potential biomarker of carotid artery stenosis, *Clin. Biochem.* 45 (16–17) (2012) 1331–1335.
- [109] K. Nonaka, N. Kume, Y. Urata, S. Seto, T. Kohno, S. Honda, et al., Serum levels of S-glutathionylated proteins as a risk-marker for arteriosclerosis obliterans, *Circ. J.* 71 (1) (2007) 100–105. (<https://pubmed.ncbi.nlm.nih.gov/17186986/>).
- [110] P.C. Rosas, R.J. Solaro, Implications of S-glutathionylation of sarcomere proteins in cardiac disorders, therapies, and diagnosis, *Front. Cardiovasc. Med. Front. Media S. A.* 9 (2023) 3856.